BIOCHEMISTRY
including biophysical chemistry & molecular biology

Article

pubs.acs.org/biochemistry

Entamoeba histolytica Rho1 Regulates Actin Polymerization through a Divergent, Diaphanous-Related Formin

Dustin E. Bosch,[†] Bing Yang,[‡] and David P. Siderovski*,[§]

[†]Department of Pharmacology and [‡]Department of Cell and Developmental Biology, The University of North Carolina at Chapel Hill, Chapel Hill, North Carolina 27599-7365, United States

[§]Department of Physiology and Pharmacology, West Virginia University School of Medicine, Morgantown, West Virginia 26506-9229, United States

Supporting Information

ABSTRACT: *Entamoeba histolytica* requires a dynamic actin cytoskeleton for intestinal and systemic pathogenicity. Diaphanous-related formins represent an important family of actin regulators that are activated by Rho GTPases. The *E. histolytica* genome encodes a large family of Rho GTPases and three diaphanous-related formins, of which EhFormin1 is known to regulate mitosis and cytokinesis in trophozoites. We demonstrate that EhFormin1 modulates actin polymerization through its formin homology 2 domain. Despite a highly divergent diaphanous autoinhibitory domain, EhFormin1 is autoinhibited by an N- and C-terminal intramolecular interaction but activated upon binding of EhRho1 to the N-terminal domain tandem. A crystal structure of the EhRho1·GTPγS−EhFormin1 complex illustrates an EhFormin1 conformation that diverges from mammalian mDia1 and lacks a secondary interaction with a Rho insert helix. The structural model also highlights residues required for specific recognition of the EhRho1 GTPase and suggests that the molecular mechanisms of EhFormin1 autoinhibition and activation differ from those of mammalian homologues.

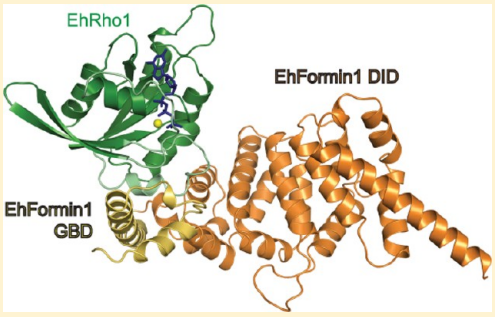

Entamoeba histolytica is the causative agent of amoebic colitis and systemic amoebiasis.[1] Infection by the parasite is spread endemically among poor populations of developing countries, although outbreaks among travelers and susceptible populations occur in the United States.[1] Water-borne *E. histolytica* cysts cycle to the trophozoite form in the human host, in some cases leading to destruction of the intestinal mucosa (amoebic colitis). If the infection is left untreated, trophozoites may enter the bloodstream, leading to systemic amoebiasis characterized by liver, lung, and brain abscesses.[2] Many cellular processes critical to *E. histolytica* pathogenesis, such as chemotaxis, adherence to intestinal epithelium, cell killing, phagocytosis, and penetration of the mucosa, are dependent on a highly dynamic actin cytoskeleton.[3−5] *E. histolytica* expresses a relatively large number of Rho family small GTPases,[6,7] conserved signaling molecules that are vital to coordination of actin cytoskeletal rearrangements.[8] Rho GTPases undergo a conformational change dominated by switch regions upon exchange of GTP for GDP, allowing engagement of specific downstream effectors.[9] Overexpression of constitutively active versions of the Rho family GTPase EhRacA or EhRacG in *E. histolytica* trophozoites impairs pathogenic processes such as phagocytosis and surface receptor capping.[10,11] However, signaling mechanisms by which the actin cytoskeleton of *E. histolytica* is regulated have not been elucidated in molecular detail.

Formins constitute a major class of proteins that directly regulate actin filament formation and thus cellular morphology, adhesion, and motility.[12] Formins promote nucleation and polymerization of unbranched actin filaments.[13] The highly conserved formin homology 2 domain (FH2) forms a head-to-tail dimer that binds to the barbed ends of actin filaments, catalyzing assembly through a processive capping mechanism.[12,14,15] The FH2 domain is commonly preceded by an unstructured, proline-rich formin homology 1 domain (FH1) that engages profilin−actin complexes, thus recruiting G-actin monomers for incorporation into a growing filament.[12] Members of the Diaphanous-related formin (DRF) subfamily also possess an N-terminal Rho GTPase binding domain (GBD) and a formin homology 3 domain (FH3) that, in turn, is composed of an Armadillo repeat-containing Diaphanous inhibitory domain (DID) and a dimerization domain.[13] C-Terminal to the FH2 domain of DRFs is a Diaphanous autoinhibitory domain (DAD) that forms intramolecular interactions with the DID, maintaining the formin in an inactive state, as best characterized structurally for DRF mDia1.[16,17] This autoinhibited conformation is released upon binding of specific Rho family GTPases to the GBD−FH3 domain tandem, likely due to active DAD displacement from its DID binding site by Rho-induced contingent folding of the GBD and by the Rho GTPase itself.[18,19] Although mDia1 primarily engages one of its activating GTPases, RhoC, through the switch regions, the last Armadillo repeat of the DID also weakly contacts the signature Rho insert helix of RhoC.[20] Mutation of residues at this secondary interface leads to reduced affinity of RhoC for mDia1, but it is

Received: July 17, 2012
Revised: October 9, 2012
Published: October 10, 2012

dx.doi.org/10.1021/bi300954g | *Biochemistry* 2012, 51, 8791−8801

unclear whether the interaction is important for formin activation per se.[14]

E. histolytica possesses a family of eight formins, among which EhFormin1−3 are Diaphanous-related.[21] EhFormin1 and -2 are expressed in trophozoites and associated with pseudopodia, pinocytic and phagocytic vesicles, and F-actin in response to serum. Both formins are also colocalized with the microtubular assembly during mitosis.[21] Overexpression of EhFormin1 increases the number of binucleated cells and nuclear DNA content, suggesting roles for EhFormin1 in mitosis and cytokinesis.[21] A recent proteomic characterization of *E. histolytica* cysts indicated that EhFormin1 is expressed during both the encysted and trophozoite life cycle stages.[22] We recently showed[7] that the GBD−FH3 domain tandem of EhFormin1 binds EhRho1 in a nucleotide state-dependent fashion, which is typical of Rho GTPase−effector interactions. Furthermore, expression of constitutively active EhRho1 in fibroblasts induced stress fiber formation,[7] suggesting that EhRho1 might regulate actin filament formation in *E. histolytica* trophozoites through EhFormin1 or other effectors. Crystal structures of EhRho1 in different nucleotide states highlighted a lack of the signature Rho insert helix,[7] suggesting that the EhRho1−EhFormin1 interaction might differ from the RhoC−mDia1 interaction.[20]

In this study, we demonstrate that EhFormin1 regulates actin polymerization through its FH2 domain. Despite considerable sequence divergence of the DAD motif and the DID motif surface expected to bind the DAD, EhFormin1 is autoinhibited by interaction between its N- and C-terminal domains. As in the case of mDia1, highly selective binding of EhRho1 to the GBD−FH3 domain tandem is sufficient to activate EhFormin1. Finally, a crystal structure of the EhRho1·GTPγS−EhFormin1 complex reveals a primary interface between EhRho1 and the EhFormin1 GBD with similarities to that of the RhoC−mDia1 complex. However, the absence of a Rho insert helix within EhRho1 and a large conformational difference in the DID of EhFormin1 compared to mDia1 illustrate the lack of a secondary EhRho1−EhFormin1 binding site, in contrast with mammalian homologues.

EXPERIMENTAL PROCEDURES

Protein Purification. EhRho1, EhRacC, EhRacD, and EhRacG were cloned from *E. histolytica* genomic DNA by polymerase chain reaction (PCR) amplification as hexahistidine-tagged open reading frame fusions, expressed in *Escherichia coli* BL21(DE3), purified by nickel affinity and gel filtration chromatography, and loaded with GTPγS as described previously for EhRho1.[7] EhFormin1 (UniProt entry C4M622) was cloned from genomic DNA, and fragments were amplified via PCR and subcloned with a tobacco etch virus (TEV) protease-cleavable hexahistidine tag using ligation-independent cloning.[23] Mutagenesis was performed using the two-PCR method.[24] All EhFormin1 fragments were expressed in *E. coli* B834 induced with 500 μM isopropyl β-D-thiogalactopyranoside (IPTG) for 14−16 h at 20 °C. For crystallization of the GBD−FH3 domain tandem, a selenium-containing derivative was produced by induction in minimal medium containing selenomethioine (Molecular Dimensions, Apopka, FL). Bacterial cells were pelleted by centrifugation and resuspended in N1 buffer composed of 50 mM Tris (pH 7.5), 250 mM NaCl, 10 mM imidazole, 1 mM DTT, and 5% (v/v) glycerol. Bacteria were lysed using pressure homogenization with an Emulsiflex (Avestin, Ottawa, ON). Cellular lysates were cleared via centrifugation at 100000*g* for 60 min at 4 °C, and the resulting supernatant was applied to a nickel-nitrilotriacetic acid (NTA) resin FPLC column (FF HisTrap crude, GE Healthcare, Piscataway, NJ) and washed with N1 buffer and 20 mM imidazole before being eluted in N1 buffer with 300 mM imidazole. EhFormin1 GBD−FH3 tandem selenomethioine protein was pooled and dialyzed overnight in imidazole-free N1 buffer with His_6-TEV protease to cleave the N-terminal affinity tag. The dialysate was then passed over a second NTA column to remove TEV protease and uncleaved protein. All EhFormin1 fragments were resolved using a calibrated size exclusion column (HiLoad 16/60 Superdex 200, GE Healthcare) in S200 buffer [50 mM HEPES (pH 8.0), 150 mM NaCl, and 5 mM DTT]. All proteins were concentrated to 0.5−2 mM and snap-frozen in a dry ice/ethanol bath for storage at −80 °C.

Actin for in vitro polymerization assays was purified from rabbit skeletal muscle acetone powder as described previously[25] and further purified via gel filtration chromatography. The actin was polymerized and conjugated with pyrene as described previously.[26] Following a final gel filtration step, the pyrene-actin was stored at 2 mg/mL and 4 °C in G buffer [2 mM Tris (pH 8.0), 0.2 mM $CaCl_2$, 0.5 mM ATP, and 5 mM DTT]. The protein concentration was determined by A_{280} measurements upon denaturation in 8 M guanidine hydrochloride, using predicted extinction coefficients for each protein (http://us.expasy.org/tools/protparam.html).

Actin Cosedimentation. Rabbit skeletal muscle actin for cosedimentation assays was purchased from Cytoskeleton, Inc. (Denver, CO). EhFormin1 FH2 domain and F-actin cosedimentation assays were conducted as previously described for talin.[27] Briefly, actin was diluted to 0.4 mg/mL in buffer containing 5 mM Tris (pH 8.0), 0.2 mM $CaCl_2$, 0.2 mM ATP, and 0.5 mM DTT and polymerized by addition of 50 mM KCl and 2 mM $MgCl_2$, followed by incubation at room temperature for 1 h. EhFormin1 fragments were incubated alone or with a 2:1 molar excess of polymerized actin in binding buffer [10 mM Tris (pH 7.0), 1 mM ATP, 0.2 mM DTT, 1 mM EGTA, 0.1 mM $CaCl_2$, and 2 mM $MgCl_2$] for 1 h at room temperature. Samples were centrifuged at 100000*g* and 20 °C for 15 min. Proteins in the supernatant and pellet fractions of each experiment were resolved by sodium dodecyl sulfate−polyacrylamide gel electrophoresis and stained with Coomassie Brilliant Blue.

Actin Polymerization in Vitro. Monomeric pyrene-actin (~20% pyrene-labeled, ~80% unlabeled) was diluted to 40 μM in buffer containing 25 μM Tris (pH 7.4) and 5 mM DTT. Twenty-five microliters of diluted pyrene-actin (final concentration of 10 μM) and various amounts of EhFormin1 fragments and/or EhRho1 were brought to a volume of 95 μL in S200 buffer [50 mM HEPES (pH 8.0), 150 mM NaCl, and 5 mM DTT]. Buffer conditions were held constant in all comparison experiments, because the ionic strength and pH are known to influence actin polymerization kinetics.[28] The fluorescence of the pyrene moiety was monitored throughout the experiment at 30 s intervals using a FluoroLog modular spectrofluorometer (Horiba, Ann Arbor, MI) with excitation and emission wavelengths of 365 and 407 nm, respectively. Following the establishment of a stable baseline fluorescence (~5 min), polymerization was initiated by addition of 5 μL of polymerization buffer [1 mM Tris (pH 7.4), 500 mM KCl, 20 mM $MgCl_2$, 2 mM ATP, and 5 mM DTT]. Polymerization was allowed to proceed for at least 1 h. The relative rate of polymerization was estimated by measuring the slope (fluorescence units per second) of the actin polymerization curve at 50% of the maximal fluorescence signal, as previously described.[28]

All slope measurements were averaged across at least three replicate experiments, and the statistical significance was determined by a Student's t test.

Surface Plasmon Resonance. SPR-based measurements of protein−protein interactions were performed on the Biacore 3000 of The University of North Carolina's Center for Structural Biology (GE Healthcare), as described previously.[7] Approximately 10000 resonance units (RUs) of purified His_6-EhFormin1 GBD−FH3 domain tandem and 5000 RUs of His_6-EhFormin1 fusion were separately immobilized on a nickel-NTA biosensor chip (GE Healthcare) using covalent capture coupling as previously described.[29] An empty surface served as a negative control. Experiments were performed in running buffer containing 50 mM HEPES (pH 7.4), 150 mM NaCl, 0.05% NP-40 alternative (Calbiochem), 50 μM EDTA, and 1 mM $MgCl_2$. For the assessment of kinetic binding properties, three injections of 5 μM EhRho1·GTPγS were performed at a rate of 10 μL/min with a 300 s dissociation phase. k_{obs} was obtained by fitting the average of three injections with a single-phase exponential association function using GraphPad Prism version 5.0. Similarly, k_{off} was obtained by fitting the average data immediately following the injections with a single-phase exponential dissociation function. Because k_{obs} is dependent on the concentration of analyte, k_{on} was derived by the relationship $k_{on} = (k_{obs} - k_{off})/(\text{analyte concentration})$. An affinity constant was derived from the kinetic data by the relationship $K_D = k_{off}/k_{on}$. For equilibrium binding analyses, multiple injections were performed with increasing concentrations of GTPγS-loaded EhRho1, EhRacC, EhRacD, and EhRacG, and an affinity constant was derived as described previously.[7]

Crystallization and Structure Determination. A complex of EhRho1·GTPγS and the selenomethionine derivative of the EhFormin1 GBD−FH3 domain tandem (amino acids 69−418) was assembled by mixing the two proteins at a 1:1 molar ratio to a total concentration of 15 mg/mL in crystallization buffer [50 mM Tris (pH 8.0), 250 mM NaCl, 2.5% (v/v) glycerol, 5 mM DTT, 50 μM GTPγS, and 1 mM $MgCl_2$] and incubation for 30 min at room temperature. Crystals of the EhRho1·GTPγS−EhFormin1 complex were obtained by vapor

Table 1. Data Collection and Refinement Statistics for the EhRho1·GTPγS−EhFormin1 Complex (PDB entry 4DVG)

Data Collection	
space group	$P6_1$
cell dimensions	
a, b, c (Å)	138.6, 138.6, 57.8
α, β, γ (deg)	90, 90, 120
	peak
wavelength (Å)	0.97954
resolution (Å)	40.0−2.6 (2.63−2.60)[a]
R_{merge} (%)	8.5 (58.0)[b]
$I/\sigma I$	15.2 (2.1)
Wilson B factor	65.0
completeness (%)	98.4 (86.0)
redundancy	9.6 (6.4)
Refinement	
resolution (Å)	35.7−2.6 (2.7−2.6)
no. of reflections	19211 (2420)
cutoff criterion	$F_{obs}/\sigma F_{obs} > 0$
R_{work}/R_{free} (%)	21.5/25.1 (33.4/37.2)
no. of atoms	
protein	3747
ligand/ion	33
water	4
B factor (Å^2)	
protein	79.5
ligand/ion	57.4
water	36.1
rmsd	
bond lengths (Å)	0.010
bond angles (deg)	1.233

[a]Values in parentheses are for the highest-resolution shell. [b]All data were collected from a single crystal.

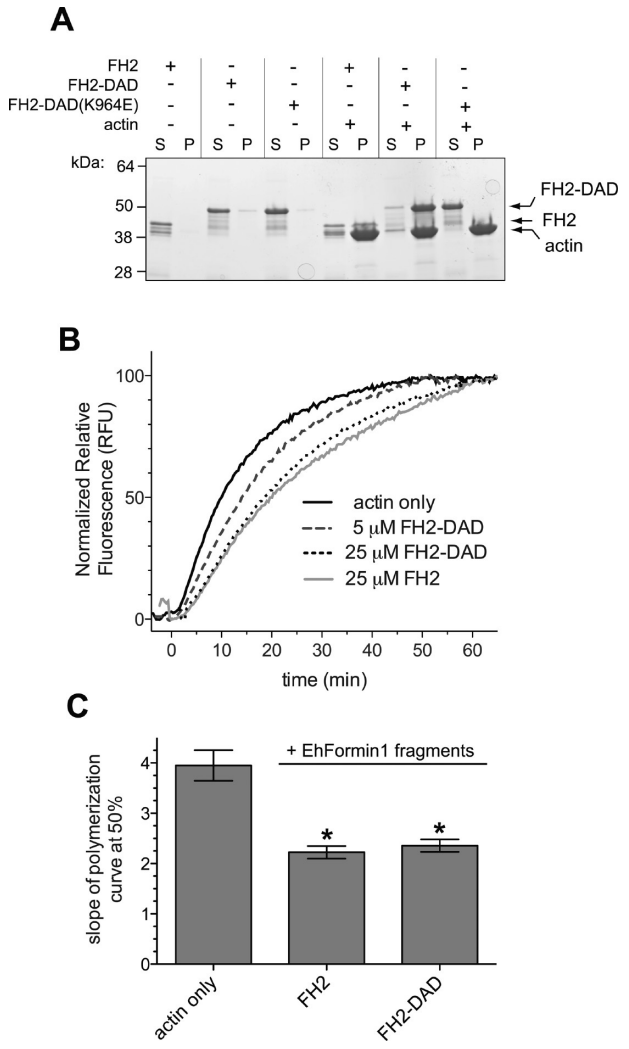

Figure 1. FH2 domain of EhFormin1 that modulates actin filament formation. (A) Actin cosedimentation assays demonstrate that the EhFormin1 FH2 domain fragment (amino acids 731−1127) and the FH2−DAD combination (amino acids 731−1182) both associate with preformed filamentous actin derived from rabbit skeletal muscle. Mutation of the conserved Lys964 that is critical for other formin FH2−actin interactions abolished cosedimentation. S and P denote the soluble and pellet fractions following high-speed centrifugation, respectively. (B) Indicated fragments of EhFormin1, each containing the FH2 domain, modulate actin polymerization in vitro, as measured by pyrene-actin polymerization assays. (C) The EhFormin1 FH2 and FH2−DAD fragments are both seen to slow actin polymerization, as quantified by measuring the slope of each fluorescence curve at 50% complete polymerization. Error bars represent the standard error of the mean (SEM) of three or more replicate experiments. Asterisks indicate a statistically significant difference from actin only ($p < 0.05$).

dx.doi.org/10.1021/bi300954g | Biochemistry 2012, 51, 8791−8801

diffusion from hanging drops at 18 °C. The protein solution was mixed in a 1:1 ratio with and equilibrated against a crystallization solution containing 18% PEG 3350, 100 mM Tris (pH 8.5), and 200 mM $MgCl_2$. Clusters of six hexagonal rod crystals grew to ~200 μm × 100 μm × 100 μm over 3 days, but diffraction was limited to >3 Å resolution. Crystal clusters were used to microseed similar crystallization experiments using the method described previously.[30] Microseeding experiments yielded single hexagonal rod crystals (~300 μm × 150 μm × 150 μm) over 5 days, exhibiting the symmetry of space group $P6_1$ ($a = b = 138.6$ Å, $c = 57.8$ Å, $\alpha = \beta = 90°$, and $\gamma = 120°$) and containing one EhRho1−EhFormin1 dimer in the asymmetric unit. For the collection of data at 100 K, crystals were serially transferred for ~1 min into a crystallization solution supplemented with 30% (v/v) glycerol in 10% increments and plunged into liquid nitrogen. Single-wavelength (0.9795 Å) anomalous diffraction data were collected at the GM/CA-CAT 23-ID-B beamline at the Advanced Photon Source (Argonne National Laboratory, Argonne, IL). Data were processed using HKL-2000.[31] Heavy atom searching, experimental phasing, and automated model building were performed with Phenix AutoSol.[32] Heavy atom searching identified 13 of 13 possible sites, and refinement yielded an estimated Bayes correlation coefficient of 51 to 2.6 Å resolution. After density modification, the estimated Bayes correlation coefficient increased to 58; ~75% of the model was constructed automatically, and the remaining portion was built manually throughout the refinement. The current model (Table 1) contains a single EhRho1−EhFormin1 dimer with EhRho1 bound to GTPγS and magnesium. Refinement was conducted against peak anomalous data with phenix.refine,[32] keeping Bijvoet pairs separate, interspersed with manual model revisions using Coot.[33] Refinement consisted of conjugate-gradient minimization and calculation of individual atomic displacement and translation/libration/screw (TLS) parameters.[34] Residues 1−20, 185, and 186 of EhRho1 and residues 69−72 and 378−418 of EhFormin1 could not be located in the electron density. The model exhibits excellent geometry as determined by MolProbity.[35] A Ramachandran analysis of protein residue backbone angles identified 93% favored, 7% allowed, and 0% disallowed. Coordinates and structure factors are deposited in the Protein Data Bank (PDB) as entry 4DVG.

RESULTS

***E. histolytica* Formin1 Modulates Actin Filament Formation.** The Diaphanous-related formins catalyze actin polymerization through the FH2 domain.[12] To examine the potential interaction of EhFormin1 with actin, two FH2 domain-containing fragments of this protein were generated and expressed from *E. coli*: FH2−DAD (amino acids 731−1182) and FH2 (amino acids 731−1127) (see Figure S1 of the Supporting Information). To determine whether the EhFormin1 FH2 domain interacts with actin, cosedimentation assays were performed[27] using rabbit skeletal muscle-derived filamentous actin. The EhFormin1 fragments FH2−DAD and FH2 were highly soluble alone, but both cosedimented with polymerized actin (Figure 1A), suggesting a direct actin−FH2 domain interaction independent of the

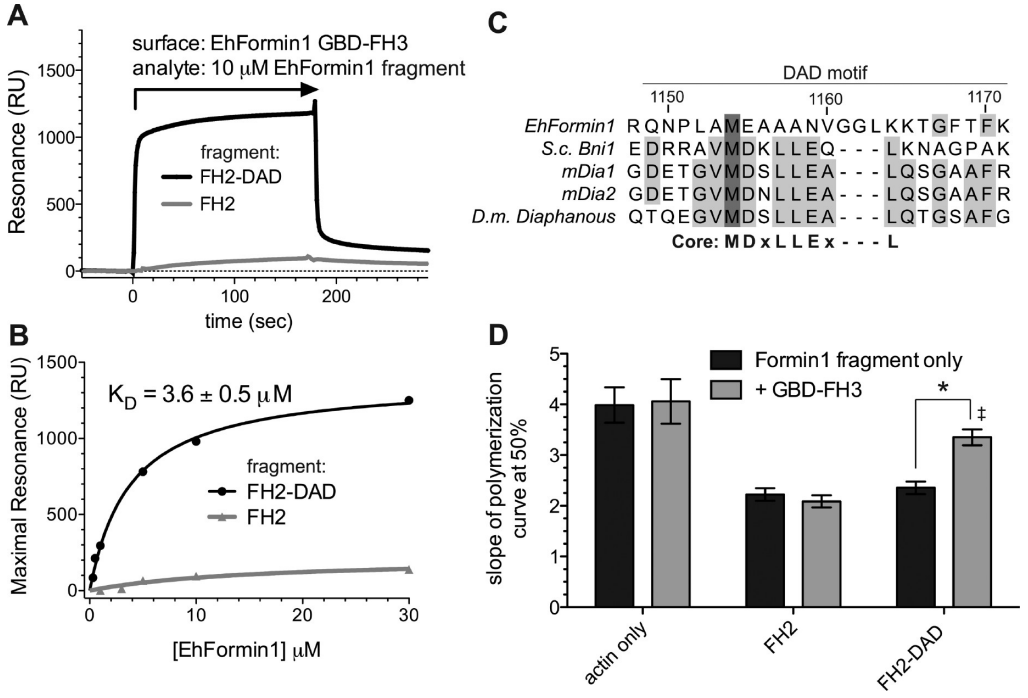

Figure 2. EhFormin1 is autoinhibited by N- and C-terminal domain interactions. (A) The N-terminal GBD−FH3 domain tandem (amino acids 69−418) of EhFormin1 binds to the C-terminal FH2−DAD tandem (amino acids 731−1182), but not the FH2 domain alone (amino acids 731−1127) as determined by surface plasmon resonance. (B) Equilibrium binding analyses revealed a DAD motif-dependent low-micromolar affinity interaction with the EhFormin1 GBD−FH3 fragment. (C) The DAD motif region, with a core motif (MDxLLExL) highly conserved among other known Diaphanous-related formins, is divergent in EhFormin1. *S.c.* denotes *Saccharomyces cerevisiae*, and *D.m.* denotes *Drosophila melanogaster*; mDia isoforms are derived from *Mus musculus*. (D) In vitro actin polymerization assays indicate a DAD motif-dependent interaction between the N- and C-terminal fragments of EhFormin1 that prevents modulation of actin polymerization. Addition of a molar excess of the GBD−FH3 domain tandem (100 μM) had no effect on the isolated FH2 domain from EhFormin1 or on actin alone. However, the GBD−FH3 tandem prevented deceleration of actin polymerization by the FH2−DAD fragment. Error bars represent the standard error of the mean (SEM) of at least three replicate experiments. The asterisk indicates a statistically significant difference ($p < 0.05$), and the double dagger indicates an indistinguishable slope compared to that of actin only.

dx.doi.org/10.1021/bi300954g | *Biochemistry* 2012, 51, 8791−8801

putative DAD motif. Mutation of a conserved surface lysine [K964 (Figure S2 of the Supporting Information)] required for actin binding by other formin FH2 domains[36] abolished actin cosedimentation, suggesting a conserved mode of FH2 domain−actin interaction (Figure 1A). To determine whether the EhFormin1−actin interaction altered actin polymerization kinetics, in vitro polymerization assays were performed with pyrene fluorophore-labeled actin (~20% labeled). The FH2 and FH2−DAD fragments each decelerated actin polymerization in a concentration-dependent fashion (Figure 1B,C), as observed by the slope of the actin polymerization curve.[28] Some isolated FH2 domains, such as that of Cdc12 in fission yeast, slow overall actin polymerization in vitro despite a positive effect on actin filament formation in a cellular context.[37] Like Cdc12, the FH2 domain of EhFormin1 may cap actin filament barbed ends and require an FH1 domain-associated profilin to accelerate polymerization.[38] However, no FH1 domain-containing EhFormin1 fragments could be obtained as a soluble recombinant protein from *E. coli*, precluding a direct test of this hypothesis. Relatively high concentrations of all EhFormin1 fragments were required to significantly alter actin polymerization kinetics, likely reflecting a low-affinity EhFormin1−actin interaction. Alignment of the EhFormin1 FH2 domain sequence with Diaphanous-related formins from other species[36] (28% identical and 48% similar to that of yeast Bni1) indicates only moderate conservation of residues known to participate in the actin interaction (Figure S2 of the Supporting Information). Similarly, the *E. histolytica* actin sequence differs significantly from that of rabbit skeletal muscle actin at FH2 domain interaction sites (not shown), suggesting that high EhFormin1 fragment concentrations may be required to overcome cross-species sequence and/or structural divergence.

EhFormin1 Is Autoinhibited by N- and C-Terminal Interactions. Other Diaphanous-related formins are maintained in an inactive conformation by interactions between the Diaphanous autoinhibitory domain (DAD motif) and a surface of the Armadillo repeat portion of the FH3 domain, also called the Diaphanous inhibitory domain (DID).[16,17] Inspection of the C-terminus of EhFormin1 revealed considerable divergence of its sequence from that of the core DAD motif conserved among other known formins (MDxLLExL) (Figure 2C). Accordingly, we wondered whether the DID−DAD autoinhibitory interaction would be conserved in the case of EhFormin1. Surprisingly, the EhFormin1 FH2−DAD long fragment was seen to interact with the N-terminal GBD−FH3 domain tandem, as determined by surface plasmon resonance (Figure 2A). This intramolecular interaction required the divergent putative DAD motif, because the FH2 domain alone did not bind the GBD−FH3 domain tandem (Figure 2A,B). To determine the effects of the GBD−FH3 domain interaction on FH2 domain-catalyzed actin filament formation, in vitro polymerization assays were conducted in the presence or absence of a molar excess of GBD−FH3 tandem protein. Addition of the GBD−FH3 tandem selectively affected the DAD motif-containing construct, returning the rate of actin polymerization in its presence to one indistinguishable from that of actin alone (Figure 2D). These results suggest that the C-terminus of EhFormin1 forms a DAD motif-dependent interaction with the N-terminal GBD−FH3 domain region that prevents the modulation of the actin polymerization rate by the FH2 domain.

Interaction of the EhFormin1 GBD−FH3 Domain Tandem with EhRho1 Reverses Autoinhibition of the FH2 Domain. In previous work,[7] we demonstrated that EhRho1 binds the GBD−FH3 domain tandem of EhFormin1 (amino acids 69−445) selectively in its GTPγS-bound, activated conformation. Because some minor degradation of that particular GBD−FH3 fragment was reported during expression and purification (e.g., see Figure 1B of ref 7), we generated multiple alternative constructs containing the GBD−FH3 region, finding that amino acids 69−418 of EhFormin1 were highly stable as a recombinant protein fragment. The residues removed from this smaller fragment (i.e., amino acids 419−445) correspond to the dimerization domain of mDia1.[20] The single-cell *E. histolytica* parasite expresses ~20 Rho family GTPases, raising the possibility of highly specific interactions between Rho GTPases and their signaling effectors. The EhFormin1 GBD−FH3 domain tandem (amino acids 69−418) was observed to interact selectively with EhRho1 to the exclusion of three other Rho GTPases that were tested (Figure 3A).

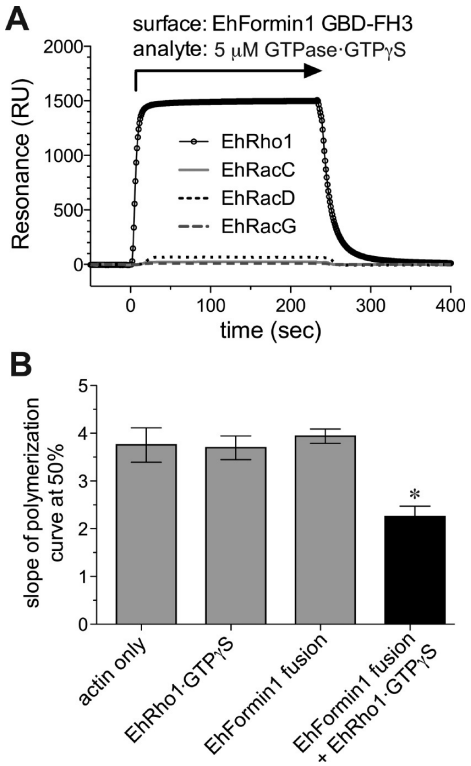

Figure 3. EhRho1 activates EhFormin1 through interaction with the GBD−FH3 domain tandem. (A) The GBD−FH3 domain tandem (amino acids 69−418) of EhFormin1, immobilized on a nickel-NTA biosensor surface, selectively engaged EhRho1·GTPγS to the exclusion of multiple other Rho family GTPases from *E. histolytica*, as measured by surface plasmon resonance. (B) The EhFormin1 fusion protein (25 μM) is apparently autoinhibited, having no measured effect on actin polymerization kinetics in vitro. While EhRho1·GTPγS alone (100 μM) did not perturb actin polymerization, it was capable of activating the EhFormin1 fusion, resulting in deceleration of actin polymerization comparable to that of the FH2−DAD fragment alone (Figure 1B,C). Error bars represent the standard error of at least three replicate experiments. The asterisk indicates statistical significance ($p < 0.05$) compared to that of actin only.

Given the apparent endoproteolytic sensitivity of its unstructured, proline-rich FH1 domain, recombinant full-length (and thus autoinhibited) EhFormin1 could not be produced and purified. To circumvent this problem, we produced a construct (hereafter termed "EhFormin1 fusion") consisting of the

dx.doi.org/10.1021/bi300954g | *Biochemistry* 2012, 51, 8791−8801

N-terminal GBD−FH3 domain tandem and the C-terminal FH2−DAD fragment, connected by a 40-residue linker to simulate the presumably flexible FH1 domain (see Figure S1 of the Supporting Information). While either the EhFormin1 fusion or EhRho1·GTPγS alone had no measurable effect on in vitro actin polymerization, the EhFormin1 fusion−EhRho1·GTPγS complex was observed to inhibit actin filament formation (Figure 3B) to a degree similar to that of the corresponding FH2−DAD construct (Figure 1C). This finding suggests that EhRho1 selectively engages the N-terminus of EhFormin1, freeing the C-terminal FH2 domain to regulate actin filament formation. Using SPR, EhRho1·GTPγS was shown to bind this EhFormin1 fusion protein with an affinity of ∼3 μM (Figure S3 of the Supporting Information).

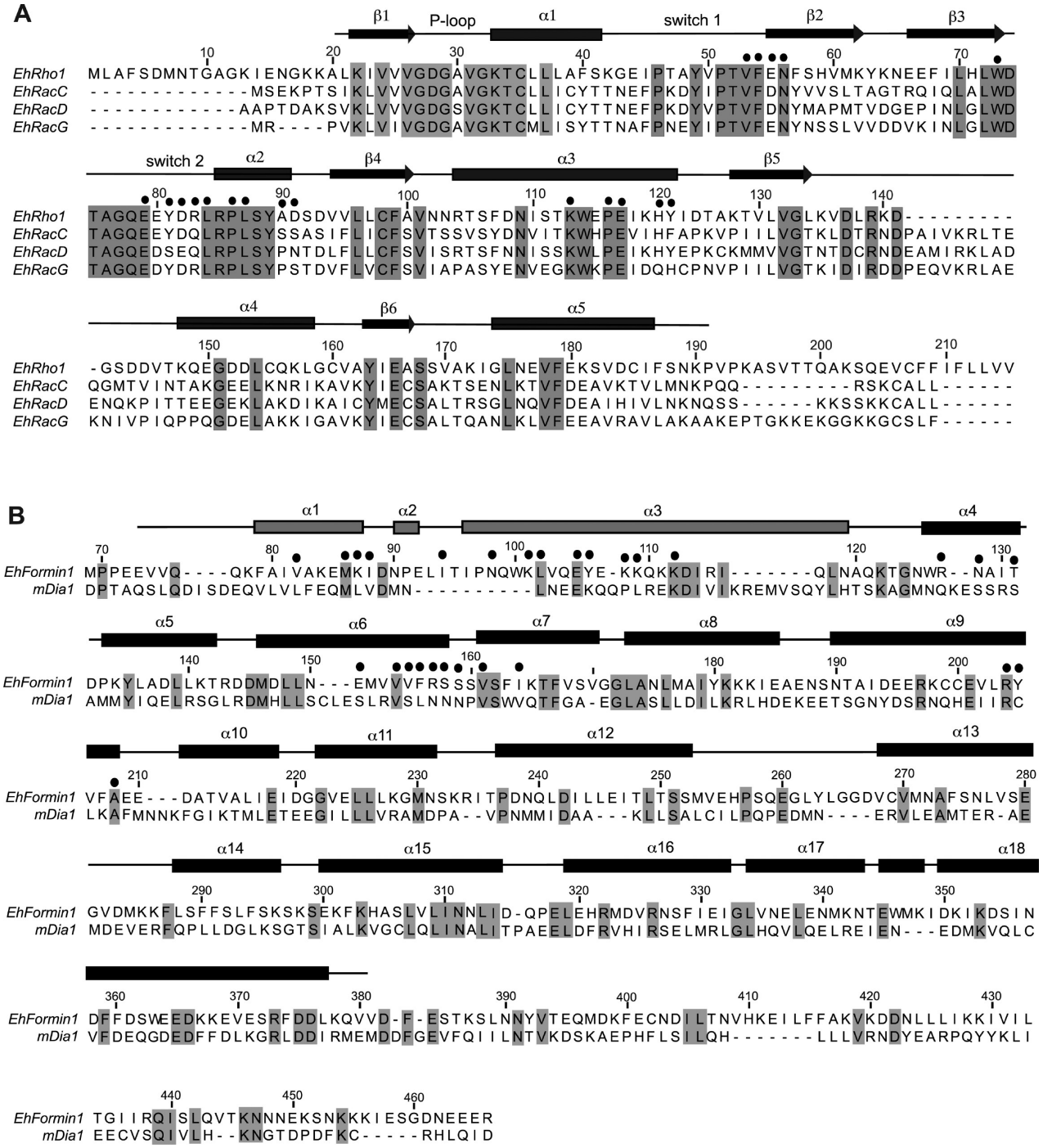

Figure 4. Comparison of sequences of Rho family GTPases and Diaphanous-related formins. (A) The protein sequence of EhRho1 is aligned with three additional *E. histolytica* Rho GTPases that do not engage EhFormin1 (Figure 3A). The secondary structure from the EhRho1·GTPγS−EhFormin1 crystal structure [PDB entry 4DVG (this work)] is diagrammed above the primary sequence. Black dots indicate residues of EhRho1·GTPγS within 1 Å of EhFormin1 in the complex. (B) The protein sequence of the EhFormin1 GBD−FH3 domain tandem is aligned with its closest mammalian homologue, mDia1. The secondary structure from the EhRho1·GTPγS−EhFormin1 crystal structure [PDB entry 4DVG (this paper)] is diagrammed above the primary sequence. Black dots indicate residues in EhFormin1 within 1 Å of EhRho1·GTPγS in the complex. All alignments were performed with ClustalW2.

dx.doi.org/10.1021/bi300954g | *Biochemistry* 2012, 51, 8791−8801

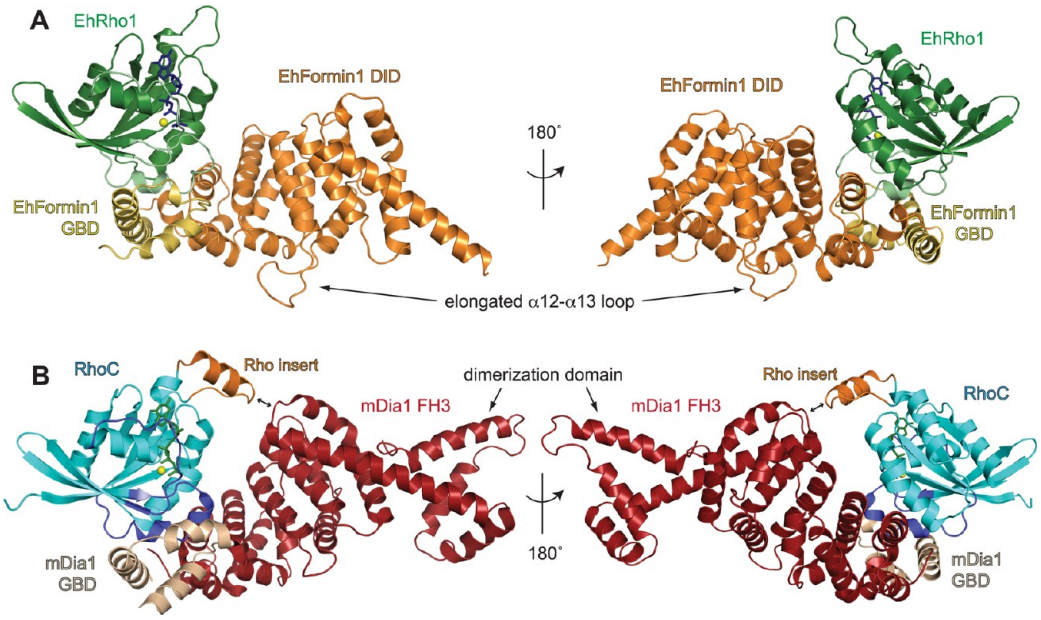

Figure 5. Crystal structure of EhRho1·GTPγS bound to the GBD−FH3 domain tandem of EhFormin1. (A) EhRho1 (dark green) in its activated state bound to GTPγS (blue sticks) engages EhFormin1 primarily through its mobile switch regions (light green) and its α3 helix. The GTPase binding domain (GBD) of EhFormin1 is colored yellow, and the Armadillo repeats of the DID are colored orange. Magnesium is shown as a yellow sphere. (B) The homologous mammalian complex between RhoC·GppNHp (cyan) and mDia1 (wheat and red) is posed in a similar configuration[20] (PDB entry 1Z2C). EhRho1 lacks a signature Rho insert helix (highlighted in orange on RhoC), and the EhFormin1 DID Armadillo repeats are rotated away from EhRho1 relative to this mammalian complex. The EhFormin1 GBD−FH3 domain tandem construct used in this study also lacks the dimerization domain portion of the FH3 domain, as shown in the RhoC−mDia1 complex.

Structural Features of the EhRho1−EhFormin1 Complex. The sequence of the GBD−FH3 domain tandem within EhFormin1 is highly divergent compared to other known Diaphanous-related formins, with mDia1 being the closest mammalian homologue (Figure 4). EhRho1 also differs significantly from mammalian Rho GTPases and other *E. histolytica* Rho GTPases (Figure 4), particularly given its lack of a signature Rho insert helix.[7] We sought a crystal structure of EhRho1 bound to EhFormin1 to allow structure-based comparison with the mammalian RhoC−mDia1 complex and to elucidate the determinants of a highly selective Rho−effector interaction. Well-diffracting crystals of the EhRho·GTPγS−EhFormin1 GBD−FH3 domain tandem were obtained with aid of microseeding (see Experimental Procedures). Molecular replacement attempts with structural models of either EhRho1 (PDB entry 3REF) or the mDia GBD−FH3 domain tandem (PDB entry 3EG5) did not produce electron density maps suitable for accurate modeling, likely given the divergent conformation of the GBD−FH3 domain tandem. A selenomethioine derivative of the EhFormin1 GBD−FH3 fragment was therefore generated, and crystallographic phases were determined by single-wavelength anomalous dispersion (SAD). For data collection and refinement statistics, see Table 1.

The overall structure of the EhRho1·GTPγS−EhFormin1 complex resembles that of the human RhoC·GppNHp−mDia1 complex[20] except that the EhFormin1 fragment used for crystallography (amino acids 69−418) lacks the dimerization domain and thus lacks the dimeric quaternary structure seen for mDia1 (Figure 5). The Armadillo repeats of the DID in EhFormin1 are rotated ∼40° away from EhRho1 relative to the conformation seen in the mammalian homologue (Figure 6). EhRho1 engages the EhFormin1 GBD and the N-terminal portion of the DID Armadillo repeats through its two mobile switch regions and its α3 helix, as also seen in mammalian homologues (Figure 5). However, the GTPase binding domain of EhFormin1 differs from that of mDia by a shortened second helix and an elongated α3 helix with clearly defined and continuous electron density. As a result of a shortened α2 helix, the GBD of EhFormin1 remains farther (∼4 Å) from the putative DAD-binding site within the DID (Figure S4 of the Supporting Information), which may indicate a slightly different mechanism of Rho-induced activation, because the contingently folded GBD of mDia1 is thought to contribute to DAD displacement by directly obstructing the DAD-binding site of the DID.[18] EhFormin1 also has an elongated α12−α13 loop relative to that of mDia1 (Figure 5). This loop is near the DAD-binding site of the DID in mDia1;[18] together with the highly divergent nature of the putative DAD motif within EhFormin1 (Figure 2), the presence of this elongated loop suggests that a unique mode of DAD-mediated autoinhibition may exist in the case of EhFormin1.

The conformation of EhRho1 in the complex is nearly identical with that we have previously reported[7] for free EhRho1·GTPγS (Cα rmsd of 0.4 Å, PDB entry 3REG) and is also similar to that of RhoC in the homologous RhoC·GppNHp−mDia1 complex (Cα rmsd of 1.5 Å, PDB entry 1Z2C) (Figure 6 and Figure S5 of the Supporting Information). The Rho insert helix of RhoC approaches the C-terminal end of the mDia1 DID (Figures 5B and 6), leading to the hypothesis that a secondary binding site (beyond the switch region−GBD interaction) may be important for mDia1 activation.[14,20] In contrast, the lack of this insert helix within EhRho1 and the relative rotation of the EhFormin1 DID indicate that such a secondary interaction is absent in the *E. histolytica* orthologues (Figures 5A and 6). An EhRho1 molecule from the adjacent asymmetric unit is interposed between the nonuniformly structured β5−α4 loop of EhRho1 and the last Armadillo repeat of the EhFormin1 DID, raising the possibility that crystal contacts could be responsible for the rotation of the DID away from EhRho1 relative to the RhoC−mDia1

dx.doi.org/10.1021/bi300954g | *Biochemistry* 2012, 51, 8791−8801

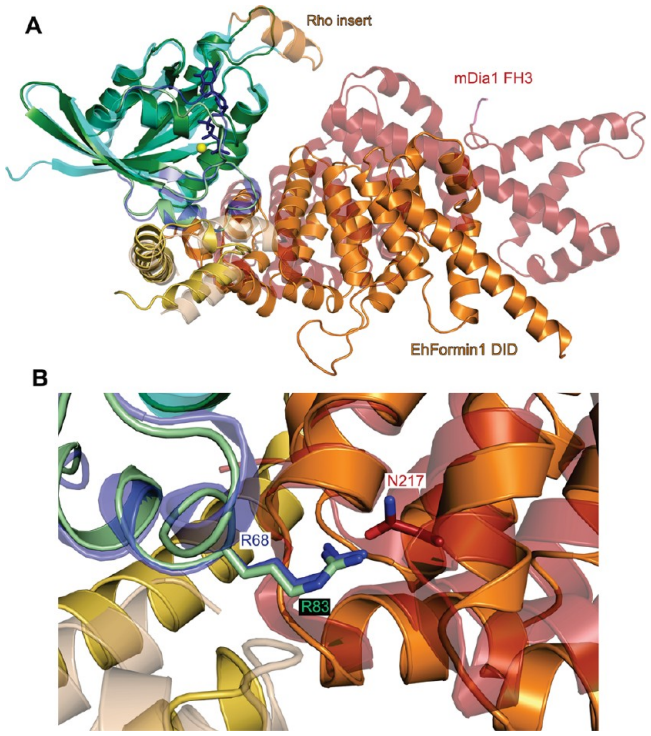

Figure 6. Structural comparison of the EhRho1−EhFormin1 complex with the mammalian RhoC−mDia1 complex. (A) The EhRho1·GTPγS−EhFormin1 complex is superimposed with the RhoC·GppNHp−mDia1 complex (PDB entry 1Z2C) using the Cα atoms of the respective Rho GTPases and colored as in Figure 5. The Rho GTPase and GBD are similar across species, but the DID exhibits a different conformation, with an ∼40° relative rotation of C-terminal Armadillo repeats. (B) The switch 2 arginines, Arg83 in EhRho1 and Arg68 in human RhoC, adopt nearly identical orientations, inserting between the GBD (yellow and wheat) and DID (orange and red). However, Arg68 of RhoC forms hydrogen bonds with Asn217 of mDia1 as well as backbone carbonyl groups, while Arg83 of EhRho1 exclusively contacts main chain carbonyl groups.

complex. However, this is unlikely given the large magnitude of rotation and the absence of significant contacts between the interposed EhRho1 and the DID; crystal contacts exist only between EhRho1 molecules in adjacent asymmetric units (see Figure S6 of the Supporting Information).

The EhRho1−EhFormin1 interface is dominated by hydrophobic interactions between the two switch regions of the GTPase and the GBD (Figure 7A). The critical EhRho1 residues at this interaction site, such as Phe54 of switch 1 and Leu84 of switch 2, are conserved across the related GTPases (Figure 4A), suggesting that these hydrophobic interactions, while important for binding, do not necessarily determine the observed specificity of EhFormin1 for EhRho1. The nonconserved Asp91 of EhRho1 is positioned to potentially form ionic contacts with EhFormin1 α2 helix residues Lys108 and Lys112 (Figure 7A). The EhRho1 α3 helix contacts the first two Armadillo repeats of the EhFormin1 DID, primarily through residues His120 and Tyr121 (Figure 7B). The imidazole ring of His120 is oriented for a hydrogen bond interaction with Glu151 of EhFormin1. Interestingly, His120 and Tyr121 are conserved in RacD, but not RacC or RacG (Figure 4A), suggesting that these two interface residues may be important for specificity. Indeed, mutation of His120 of EhRho1 to Gln, the analogous residue in EhRacG, drastically reduced the affinity for the EhFormin1 GBD−FH3 domain tandem as measured by SPR (Figure 7D). Finally, EhRho1 switch 2 residue Arg83 is inserted into a groove between the GBD and the DID, a region of slightly negative charge as indicated by vacuum electrostatic calculations (Figure 7C). Arg83 is within hydrogen bonding distance of multiple exposed peptide backbone carbonyl groups in this region [Phe156 and Arg157 (see Figure S7 of the Supporting Information)]. Arg83 of EhRho1 corresponds to Arg68 of human RhoC, which engages its formin effector in a strikingly similar fashion (Figure 6B) and is required for high-affinity interaction.[18] However, RhoC Arg68 forms hydrogen bonds with the side chain of mDia N217, while EhRho1 Arg83 is exclusively within hydrogen bonding distance of backbone carbonyl groups (Figure 6 and Figure S7 of the Supporting Information). This arginine is also present in EhRacG, but not other Rho family GTPases (Figure 4A), implicating this particular residue as a likely determinant of specificity for the EhRho1−EhFormin1 interaction. Mutation of EhRho1 Arg83 to the corresponding Gln in EhRacC and EhRacD drastically reduced the affinity for EhFormin1 [K_D > 100 μM compared to ∼3 μM for wild-type EhRho1 (Figure 7D)].

DISCUSSION

The isolated FH2 domain of EhFormin1 was observed to slow actin polymerization in vitro, a phenomenon also exhibited by the corresponding domain from fission yeast Cdc12,[37] suggesting a possibly similar actin barbed-end-capping interaction. Other formin regions mediate interactions with proteins that can also influence its activation state as an agent of actin polymerization.[39] Perhaps the best studied is the interaction of actin-bound profilin with the proline-rich FH1 domain.[40] Profilins can increase the rate of actin filament elongation by formins, possibly by increasing the local concentration of actin monomers to be included in the growing filament.[15] In the case of fission yeast Cdc12, the FH1 domain and associated profilin are required, in combination with the FH2 domain, for acceleration of actin polymerization.[38] While in vitro actin polymerization assays with EhFormin1 fragments provide important mechanistic insights into the activity of the isolated protein, it is important to note that the full-length protein in a cellular context is likely also modulated by subcellular localization and interactions with multiple other proteins. A limitation of the pyrene-actin polymerization assay used in this study is its inability to differentiate the effects of EhFormin1 on nucleation of new actin filaments versus accelerated elongation of existing filaments. Nucleation and elongation are catalyzed with varying efficiencies among formins,[12] and further studies are thus necessary to elucidate fully the mechanisms by which EhFormin1 modulates actin polymerization.

DRFs are commonly autoinhibited by an intramolecular interaction between the N-terminal DID and the C-terminal DAD, consisting of a core MDxLLExL motif followed by a polybasic region.[19] However, the C-terminus of EhFormin1 contains a highly divergent segment (MExAANxG) corresponding to the core DAD motif, suggesting a potentially unique mode of regulation. Despite poor conservation of the putative DID−DAD interface, the N- and C-terminal fragments of EhFormin1 were seen to bind one another in a DAD-dependent fashion, resulting in inhibition of FH2 domain-mediated modulation of actin polymerization. Furthermore, a fusion protein containing the N-terminal GBD−FH3 tandem and the C-terminal FH2−DAD tandem mimicked the presumably autoinhibited state of full-length EhFormin1, having no measurable effect on actin polymerization kinetics; binding of activated EhRho1·GTPγS to

dx.doi.org/10.1021/bi300954g | Biochemistry 2012, 51, 8791−8801

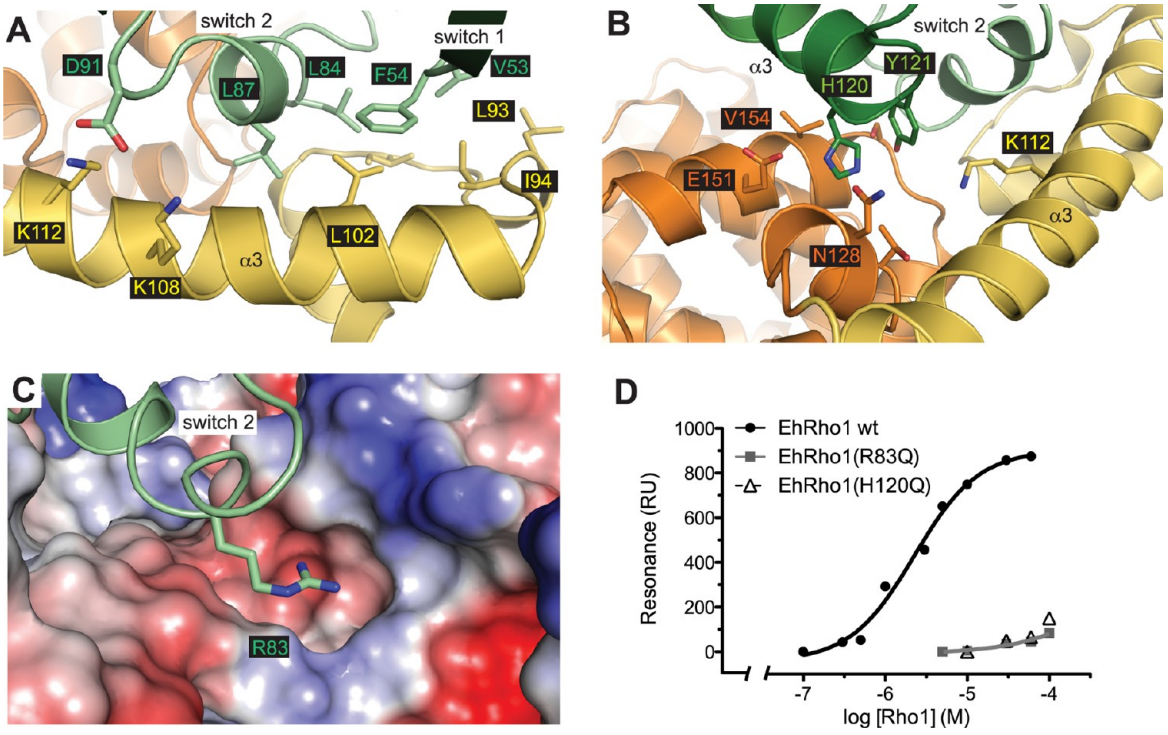

Figure 7. Structural determinants of EhRho1−EhFormin1 binding specificity. (A) The EhRho1·GTPγS−EhFormin1 interface is dominated by a hydrophobic surface burial involving the switch regions of EhRho1 (green) and the EhFormin1 GBD (yellow). Key hydrophobic residues are shown as sticks. EhRho1 Asp91 is also in position to form an ionic interaction with Lys108 or Lys112 of EhFormin1. (B) The α3 helix of EhRho1 (green) also contributes to the binding interface, with His120 and Tyr121 inserted between the GBD α3 helix (yellow) and the N-terminal portion of the DID (orange). The imidazole ring of His120 is oriented for hydrogen bonding with Glu151 of EhFormin1. (C) EhRho1 switch 2 residue Arg83 inserts into a groove between the GBD and DID of EhFormin1 (shown as an electrostatic surface). The guanidinium group of Arg83 resides near an area of relative negative charge (red surface) and is within hydrogen bonding distance of multiple backbone carbonyl groups (see Figure S7 of the Supporting Information). (D) Wild-type EhRho1 binds the EhFormin1 GBD−FH3 domain tandem, as measured by surface plasmon resonance. Mutation of either Arg83 to the corresponding glutamine in EhRacC and EhRacD or His120 to an EhRacG-like glutamine resulted in a >100-fold affinity reduction.

the GBD−FH3 region reversed the apparent autoinhibition of the EhFormin1 fusion, suggesting that the EhRho1−EhFormin1 interaction is sufficient to free the FH2 domain for modulation of actin polymerization.

The crystal structure in this study provides only the second exemplary snapshot of an interaction between a Rho GTPase and formin effector. Thus, a comparison of the *E. histolytica* and human Rho−formin complexes reveals consistent structural features that are conserved across species and likely of shared importance for Rho-mediated activation of formins, as well as differences that may reflect properties of individual proteins, such as formin specificity for particular Rho GTPases. Our structural model of the EhRho1−EhFormin1 complex reveals an interface similar to that of the human RhoC−mDia1 complex despite a distant evolutionary relationship as evidenced by substantial sequence divergence. The GTPase binding domain of EhFormin1 is quite similar to that of mDia1, with a predominant hydrophobic patch engaging the switch regions of EhRho1.[20] Arg83 of EhRho1 projects into a relatively negatively charged groove between the GBD and DID in a manner highly homologous to that of Arg68 of RhoC.[20] However, the EhRho1 Arg83 residue forms hydrogen bonds exclusively with backbone carbonyl groups rather than asparagine side chains, as seen in the mammalian homologue.[20] The EhRho1 switch 2 residue Arg83 and the buried side chains of His120 and Tyr121 on the α3 helix of EhRho1 are important determinants of Rho GTPase specificity in binding EhFormin1. EhRacC and EhRacD lack the critical switch 2 arginine, while EhRacG lacks the histidine-tyrosine tandem; all three of these Rac subfamily GTPases are unable to bind EhFormin1. Furthermore, mutation of EhRho1 residue Arg83 to the corresponding EhRacC/D glutamine or His120 to the EhRacG-like glutamine each reduced the affinity of EhRho1 for EhFormin1 by >100-fold. Such strict specificity of Rho GTPase and effector interactions is likely of particular importance in *E. histolytica* where at least 19 Rho family GTPases are apparently expressed in a single cell.[7]

Several lines of evidence suggest that the mechanisms of EhFormin1 autoinhibition and its activation by EhRho1 may differ significantly from that of the well-studied mDia1 homologue.[16,17] There is poor EhFormin1 sequence conservation in the putative core DAD motif and DAD-binding surface on the DID, and EhFormin1 has a uniquely elongated α12−α13 loop near the putative DID−DAD interaction site. Furthermore, the GBD of EhFormin1 has a shortened α2 helix that would not directly obstruct the DAD-binding surface on the DID as modeled for mDia1 (Figure S4 of the Supporting Information).[18] Finally, EhRho1 lacks a Rho insert helix and does not approach the C-terminus of the DID, indicating that a secondary EhRho1−EhFormin1 interaction between these two regions does not exist, in contrast with the RhoC−mDia1 interaction.

Previous studies of EhFormin1 in the context of *E. histolytica* trophozoites,[21] together with our findings (ref 7 and this paper), suggest that an EhRho1−EhFormin1 signaling axis may be important for formation of complex actin structures within

dx.doi.org/10.1021/bi300954g | *Biochemistry* 2012, 51, 8791−8801

pseudopodia and phagocytic and pinocytic vesicles, particularly in response to extracellular cues such as serum factors. EhFormin1 also apparently exerts effects on trophozoite mitosis and cytokinesis.[21] Interestingly, both EhRho1 and EhFormin1 are enriched in *E. histolytica* uropods,[41] suggesting that the GTPase−effector pair may also regulate actin polymerization at the trailing edge during trophozoite migration and/or surface receptor capping critical for immune response evasion.[5] Knowledge of the structural determinants defining the EhRho1−EhFormin1 interaction, and of its differences from the mammalian GTPase−formin interaction (Figure 7), should assist in understanding the contributions of this actin polymerization pathway to *E. histolytica* infectivity and invasiveness.

■ ASSOCIATED CONTENT

Ⓢ Supporting Information

Protein sequence information and constructs used in this study, supporting EhRho1−EhFormin1 fusion binding experiments, additional comparison of the EhRho1−EhFormin1 complex to previous structures, an analysis of crystal contacts, and an example electron density map. This material is available free of charge via the Internet at http://pubs.acs.org.

■ AUTHOR INFORMATION

Corresponding Author

*Address: 3051 Robert C. Byrd Health Sciences Center, West Virginia University School of Medicine, Morgantown, WV 26506-9229. Telephone: (304) 293-4991. E-mail: dpsiderovski@hsc.wvu.edu.

Funding

Work in the Siderovski lab was supported by National Institutes of Health Grant GM082892, and D.E.B. was supported by an individual National Research Service Award predoctoral fellowship from the National Institute of Diabetes and Digestive and Kidney Diseases (F30DK091978).

Notes

The authors declare no competing financial interest.

■ ACKNOWLEDGMENTS

We thank the lab of Dr. Ken Jacobson [The University of North Carolina at Chapel Hill (UNC)] for providing pyrene-actin, Dr. John Sondek (UNC) for access to his fluorometer, and Dr. Kevin Slep and Jaime Campbell (UNC) for insights into formin-mediated cytoskeletal dynamics. We thank the UNC Center for Structural Biology for access to SPR and crystallography equipment. We also thank the Advanced Photon Source (GM/CA-CAT 23-IDB beamline) at Argonne National Laboratory.

■ ABBREVIATIONS

DID, Diaphanous inhibitory domain; DAD, Diaphanous autoinhibitory domain; FH1, formin homology 1; FH2, formin homology 2; FH3, formin homology 3; GBD, GTPase binding domain; rmsd, root-mean-square deviation; RU, resonance unit; SAD, single-wavelength anomalous dispersion; SPR, surface plasmon resonance.

■ REFERENCES

(1) Haque, R., Huston, C. D., Hughes, M., Houpt, E., and Petri, W. A., Jr. (2003) Amebiasis. *N. Engl. J. Med. 348*, 1565−1573.

(2) Ravdin, J. I. (2000) *Amoebiasis*, Vol. 2, Imperial College Press, London.

(3) Voigt, H., and Guillen, N. (1999) New insights into the role of the cytoskeleton in phagocytosis of *Entamoeba histolytica*. *Cell. Microbiol. 1*, 195−203.

(4) Guillen, N. (1996) Role of signalling and cytoskeletal rearrangements in the pathogenesis of *Entamoeba histolytica*. *Trends Microbiol. 4*, 191−197.

(5) Meza, I., Talamas-Rohana, P., and Vargas, M. A. (2006) The cytoskeleton of *Entamoeba histolytica*: Structure, function, and regulation by signaling pathways. *Arch. Med. Res. 37*, 234−243.

(6) Lohia, A., and Samuelson, J. (1996) Heterogeneity of *Entamoeba histolytica rac* genes encoding p21rac homologues. *Gene 173*, 205−208.

(7) Bosch, D. E., Wittchen, E. S., Qiu, C., Burridge, K., and Siderovski, D. P. (2011) Unique structural and nucleotide exchange features of the Rho1 GTPase of *Entamoeba histolytica*. *J. Biol. Chem. 286*, 39236−39246.

(8) Ridley, A. J., and Hall, A. (1992) The small GTP-binding protein rho regulates the assembly of focal adhesions and actin stress fibers in response to growth factors. *Cell 70*, 389−399.

(9) Wennerberg, K., and Der, C. J. (2004) Rho-family GTPases: It's not only Rac and Rho (and I like it). *J. Cell Sci. 117*, 1301−1312.

(10) Ghosh, S. K., and Samuelson, J. (1997) Involvement of p21racA, phosphoinositide 3-kinase, and vacuolar ATPase in phagocytosis of bacteria and erythrocytes by *Entamoeba histolytica*: Suggestive evidence for coincidental evolution of amebic invasiveness. *Infect. Immun. 65*, 4243−4249.

(11) Guillen, N., Boquet, P., and Sansonetti, P. (1998) The small GTP-binding protein RacG regulates uroid formation in the protozoan parasite *Entamoeba histolytica*. *J. Cell Sci. 111* (Part 12), 1729−1739.

(12) Chesarone, M. A., DuPage, A. G., and Goode, B. L. (2010) Unleashing formins to remodel the actin and microtubule cytoskeletons. *Nat. Rev. Mol. Cell Biol. 11*, 62−74.

(13) Higgs, H. N. (2005) Formin proteins: A domain-based approach. *Trends Biochem. Sci. 30*, 342−353.

(14) Lammers, M., Meyer, S., Kuhlmann, D., and Wittinghofer, A. (2008) Specificity of interactions between mDia isoforms and Rho proteins. *J. Biol. Chem. 283*, 35236−35246.

(15) Schonichen, A., and Geyer, M. (2010) Fifteen formins for an actin filament: A molecular view on the regulation of human formins. *Biochim. Biophys. Acta 1803*, 152−163.

(16) Nezami, A., Poy, F., Toms, A., Zheng, W., and Eck, M. J. (2010) Crystal structure of a complex between amino and carboxy terminal fragments of mDia1: Insights into autoinhibition of diaphanous-related formins. *PLoS One 5*, e12992.

(17) Otomo, T., Tomchick, D. R., Otomo, C., Machius, M., and Rosen, M. K. (2010) Crystal structure of the Formin mDia1 in autoinhibited conformation. *PLoS One 5*, e12896.

(18) Lammers, M., Rose, R., Scrima, A., and Wittinghofer, A. (2005) The regulation of mDia1 by autoinhibition and its release by Rho*GTP. *EMBO J. 24*, 4176−4187.

(19) Nezami, A. G., Poy, F., and Eck, M. J. (2006) Structure of the autoinhibitory switch in formin mDia1. *Structure 14*, 257−263.

(20) Rose, R., Weyand, M., Lammers, M., Ishizaki, T., Ahmadian, M. R., and Wittinghofer, A. (2005) Structural and mechanistic insights into the interaction between Rho and mammalian Dia. *Nature 435*, 513−518.

(21) Majumder, S., and Lohia, A. (2008) Entamoeba histolytica encodes unique formins, a subset of which regulates DNA content and cell division. *Infect. Immun. 76*, 2368−2378.

(22) Ali, I. K., Haque, R., Siddique, A., Kabir, M., Sherman, N. E., Gray, S. A., Cangelosi, G. A., and Petri, W. A., Jr. (2012) Proteomic Analysis of the Cyst Stage of *Entamoeba histolytica*. *PLoS Neglected Trop. Dis. 6*, e1643.

(23) Stols, L., Gu, M., Dieckman, L., Raffen, R., Collart, F. R., and Donnelly, M. I. (2002) A new vector for high-throughput, ligation-independent cloning encoding a tobacco etch virus protease cleavage site. *Protein Expression Purif. 25*, 8−15.

(24) Ho, S. N., Hunt, H. D., Horton, R. M., Pullen, J. K., and Pease, L. R. (1989) Site-directed mutagenesis by overlap extension using the polymerase chain reaction. *Gene 77*, 51−59.

(25) Spudich, J. A., and Watt, S. (1971) The regulation of rabbit skeletal muscle contraction. I. Biochemical studies of the interaction of the tropomyosin-troponin complex with actin and the proteolytic fragments of myosin. *J. Biol. Chem. 246*, 4866−4871.
(26) Cooper, J. A., Walker, S. B., and Pollard, T. D. (1983) Pyrene actin: Documentation of the validity of a sensitive assay for actin polymerization. *J. Muscle Res. Cell Motil. 4*, 253−262.
(27) Srivastava, J., and Barber, D. (2008) Actin co-sedimentation assay; for the analysis of protein binding to F-actin. *J. Visualized Exp.*, 690.
(28) Harris, E. S., and Higgs, H. N. (2006) Biochemical analysis of mammalian formin effects on actin dynamics. *Methods Enzymol. 406*, 190−214.
(29) Kimple, A. J., Muller, R. E., Siderovski, D. P., and Willard, F. S. (2010) A capture coupling method for the covalent immobilization of hexahistidine tagged proteins for surface plasmon resonance. *Methods Mol. Biol. 627*, 91−100.
(30) Luft, J. R., and DeTitta, G. T. (1999) A method to produce microseed stock for use in the crystallization of biological macromolecules. *Acta Crystallogr. D55*, 988−993.
(31) Otwinowski, Z., and Minor, W. (1997) Processing of X-ray Diffraction Data Collected in Oscillation Mode. In *Methods in Enzymology*, pp 307−326, Academic Press, New York.
(32) Adams, P. D., Afonine, P. V., Bunkoczi, G., Chen, V. B., Davis, I. W., Echols, N., Headd, J. J., Hung, L. W., Kapral, G. J., Grosse-Kunstleve, R. W., McCoy, A. J., Moriarty, N. W., Oeffner, R., Read, R. J., Richardson, D. C., Richardson, J. S., Terwilliger, T. C., and Zwart, P. H. (2010) PHENIX: A comprehensive Python-based system for macromolecular structure solution. *Acta Crystallogr. D66*, 213−221.
(33) Emsley, P., Lohkamp, B., Scott, W. G., and Cowtan, K. (2010) Features and development of Coot. *Acta Crystallogr. D66*, 486−501.
(34) Painter, J., and Merritt, E. A. (2006) Optimal description of a protein structure in terms of multiple groups undergoing TLS motion. *Acta Crystallogr. D62*, 439−450.
(35) Chen, V. B., Arendall, W. B., III, Headd, J. J., Keedy, D. A., Immormino, R. M., Kapral, G. J., Murray, L. W., Richardson, J. S., and Richardson, D. C. (2010) MolProbity: All-atom structure validation for macromolecular crystallography. *Acta Crystallogr. D66*, 12−21.
(36) Otomo, T., Tomchick, D. R., Otomo, C., Panchal, S. C., Machius, M., and Rosen, M. K. (2005) Structural basis of actin filament nucleation and processive capping by a formin homology 2 domain. *Nature 433*, 488−494.
(37) Shemesh, T., and Kozlov, M. M. (2007) Actin polymerization upon processive capping by formin: A model for slowing and acceleration. *Biophys. J. 92*, 1512−1521.
(38) Kovar, D. R., Kuhn, J. R., Tichy, A. L., and Pollard, T. D. (2003) The fission yeast cytokinesis formin Cdc12p is a barbed end actin filament capping protein gated by profilin. *J. Cell Biol. 161*, 875−887.
(39) Aspenstrom, P. (2010) Formin-binding proteins: Modulators of formin-dependent actin polymerization. *Biochim. Biophys. Acta 1803*, 174−182.
(40) Kursula, P., Kursula, I., Massimi, M., Song, Y. H., Downer, J., Stanley, W. A., Witke, W., and Wilmanns, M. (2008) High-resolution structural analysis of mammalian profilin 2a complex formation with two physiological ligands: The formin homology 1 domain of mDia1 and the proline-rich domain of VASP. *J. Mol. Biol. 375*, 270−290.
(41) Marquay Markiewicz, J., Syan, S., Hon, C. C., Weber, C., Faust, D., and Guillen, N. (2011) A proteomic and cellular analysis of uropods in the pathogen *Entamoeba histolytica*. *PLoS Neglected Trop. Dis. 5*, e1002.